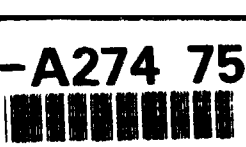

1 AGENCY USE ONLY	2 REPORT DATE	3 TYPE/DATES COVERED
	1992	

4 TITLE AND SUBTITLE MOLECULAR DYNAMICS SIMULATION OF SEDIMENTATION

5 FUNDING NUMBERS

6 AUTHOR R A J BORG, D A JONES AND S G LAMBRAKOS

7 FORMING ORG NAMES/ADDRESSES DEFENCE SCIENCE AND TECHNOLOGY ORGANIZATION, MATERIALS RESEARCH LABORATORY, PO BOX 50, ASCOT VALE VICTORIA 3032 AUSTRALIA

8 PERFORMING ORG. REPORT NO

09 SPONSORING/MONITORING AGENCY NAMES AND ADDRESSES

11 SUPPLEMENTARY NOTES

12 DISTRIBUTION/AVAILABILITY STATEMENT

DISTRIBUTION STATEMENT A

12B DISTRIBUTION CODE

13. ABSTRACT (MAX 200 WORDS): THIS PAPER DESCRIBES THE APPLICATION A MOLECULAR DYNAMICS (MD) COMPUTER SIMULATION TECHNIQUE WHICH W AS USED TO STUDY THE SEDIMENTATION PROCESS. WE CONSIDERED N MACROSCOPIC SIZE PARTICLES IN A VISCOUS FLUID SUBJECT TO GRAVITY AND INTERPARTICLE FORCES. CALCULATIONS WERE PERFORMED FOR THREE DIFFERENT PARTICLE SIZES FOR BOTH MONOMODAL AND BIMODAL PARTICLE SIZE DISTRIBUTIONS. THE MONOMODAL RESULTS SHOWED A SIZE DEPENDENT PACKING EFFECT. WHIEL WITH BIMODAL DISTRIBUTIONS FRACTIONATION WAS FOUND TO OCCUR, GIVING RISE TO A LAYER OF SMALLER PARTICLES ON THE TOPE OF THE SEDIMENT.

14 SUBJECT TERMS

15 NUMBER OF PAGES

8

16 PRICE CODE

17 SECURITY CLASS.REPORT	18 SEC CLASS PAGE	19 SEC CLASS ABST.	20 LIMITATION OF ABSTRACT
UNCLASSIFIED	UNCLASSIFIED		UNCLASSIFIED

Computational Techniques & Applications: CTAC-91
B.J. Noye, B.R. Benjamin & L.H. Colgan (Editors)

MOLECULAR DYNAMICS SIMULATION OF SEDIMENTATION

R.A.J. Borg, D.A. Jones and S.G. Lambrakos*

Materials Research Laboratory, D.S.T.O., Melbourne, Australia 3032

* *Naval Research Laboratory, Washington, D.C., USA*

1. INTRODUCTION

Composition B is a widely used military explosive consisting of a 60/40 mixture of RDX (hexahydrotrinitro-s-triazine) and TNT (trinitrotoluene). Ordnance is filled by a casting process in which Composition B is heated above the melting point of TNT (82°C), poured into the shell, and allowed to cool and solidify. During this process the heated mixture is essentially a suspension of solid RDX particles in liquid TNT, and sedimentation of RDX can occur in the shell during cooling and solidification of the TNT. The sedimentation will lead to localized regions of higher RDX content and higher sensitivity, because RDX is more sensitive to initiation than TNT.

This paper describes the application of a Molecular Dynamics (MD) computer simulation technique which was used to study the sedimentation process. We considered N macroscopic size spherical particles in a viscous fluid subject to gravity and interparticle forces. Calculations were performed for three different particle sizes for both monomodal and bimodal particle size distributions. The monomodal results showed a size dependent packing effect, while with bimodal distributions fractionation was found to occur, giving rise to a layer of smaller particles on the top of the sediment.

The CPU time for the initial version of our code varied as N^2 because of the nearest neighbours problem. This limited the maximum number of particles in our simulations to slightly more than 200, and so later versions of the code included a Monotonic Lagrangian Grid (MLG) algorithm (Boris, 1986) to keep track of nearest neighbour relationships and reduce the computational time to an order N dependence. We briefly describe the implementation of the MLG into our sedimentation code and the improvement in performance which was obtained.

2. MOLECULAR DYNAMICS MODEL

In MD calculations the forces on all particles are calculated and the particles are moved according to Newton's equations of motion. The initial state of the sedimenting system consists of N particles dispersed homogeneously in a viscous medium and subject to gravity and interparticle forces. The final state consists of a completely sedimented system in which none of the particles has any significant motion.

The important forces in a sedimentation process are viscosity, gravity, interparticle forces and particle/floor forces. The magnitude of the viscous force on a spherical particle is given by

$$\mathbf{F}_i^{visc} = -6\pi\eta r_i \mathbf{v}_i \qquad (1)$$

where η is the liquid phase viscosity, r_i is the radius of particle i and $\mathbf{v}_i$ the velocity. This force acts in a direction opposite to the direction of motion of the particle.

$\epsilon \times 10^{14}$	Particle Radius (μm)		
(J)	30	50	100
30	0.473	1.50	10.4
50	1.50	3.65	18.5
100	10.4	18.5	58.4

Table 1: ϵ values used in the interparticle force calculation.

$\sigma \times 10^{5}$	Particle Radius (μm)		
(m)	30	50	100
30	14.7	19.6	31.9
50	19.6	24.5	36.8
100	31.9	36.8	49.0

Table 2: σ values used in the interparticle force calculation.

Radius (μm)	30	50	100
K ($N.m^{13}$)	3.54×10^{-68}	1.25×10^{-64}	8.22×10^{-60}

Table 3: K values used in the particle/floor force calculation.

The interparticle forces describe the interaction between particles. Here, the particles are assumed to be spherical "soft" spheres. A soft sphere model is necessary to overcome numerical stability problems as well as reducing particle overlap. A truncated Lennard-Jones 12-6 type potential proved to be the most suitable and the force is given by

$$\mathbf{F}_{ij} = 4\epsilon_{ij}\left(\frac{12\sigma_{ij}^{12}}{r_{ij}^{13}} - \frac{6\sigma_{ij}^{6}}{r_{ij}^{7}}\right)\hat{\mathbf{d}} \tag{2}$$

where r_{ij} is the interparticle distance, ϵ_{ij} and σ_{ij} are constants for pair (i,j) and $\hat{\mathbf{d}}$ is a unit vector along the interparticle line.

A particle-floor force is needed between the particles and the bottom of the container. The form of this force was taken to be

$$\mathbf{F}_i^{floor} = \frac{K_i}{r_i^{floor^{13}}}\hat{\mathbf{k}} \tag{3}$$

where r_i^{floor} is the distance between particle i and the bottom of the container, K_i is a constant for particle type i and $\hat{\mathbf{k}}$ is a unit vector in the Z direction. The form of this potential is basically the repulsive part of Equation (2) and was chosen for consistency, as well as its success in providing an adequate description of the bottom boundary.

Values of ϵ_{ij} and σ_{ij} can be obtained in the literature for atoms and molecules. However, values for macroscopic particles like those used in this study are not readily available. The values used here have been chosen somewhat arbitrarily but satisfy the required conditions well, i.e. the particles behave as soft spheres. K values are also assigned in a similar fashion. Tables 1, 2 and 3 list values of ϵ_{ij}, σ_{ij} and K_i used in this work. The results we obtained were found not to be sensitive to the values used.

The effect of Brownian motion on the sedimenting particles has not been included as the particle sizes considered here are large enough for it to be neglected. A simple criterion for the neglect of Brownian motion is that the particle Péclet number be much larger than unity (Bossis and Brady, 1984). For the system considered here this will be the case provided the particle number is greater than 1μm. The smallest particle radius considered here is 30μm, and so Brownian motion has not been included in the calculation.

The total force on a particle is therefore given by

$$\mathbf{F}_i = m_i\mathbf{a}_i = \sum_{\substack{j=1 \\ (j\neq i)}}^{N} \mathbf{F}_{ij} + m_i\mathbf{g} - 6\pi\eta r_i\mathbf{v}_i + \mathbf{F}_i^{floor} \tag{4}$$

where N is the number of particles, $\mathbf{v}_i$ is the velocity of particle i and $\mathbf{a}_i$ the acceleration.

We integrate the equations of motion using the Verlet equations in the following form

$$\mathbf{v}_i(t) = \frac{1}{2\Delta t}\left(\mathbf{r}_i(t+\Delta t) - \mathbf{r}_i(t-\Delta t)\right) \tag{5}$$

$$\mathbf{r}_i(t+\Delta t) = 2\mathbf{r}_i(t) - \mathbf{r}_i(t-\Delta t) + \mathbf{a}_i(t)\Delta t^2 \tag{6}$$

To calculate $\mathbf{r}_i(t+\Delta t)$, $\mathbf{a}_i(t)$ must be known, and to calculate $\mathbf{a}_i(t)$ from Equation (4) we need $\mathbf{v}_i(t)$ which, in turn, is dependent on $\mathbf{r}_i(t+\Delta t)$. This difficulty can be overcome as follows; Equation (4) can be written (in one dimension) as

$$\frac{d^2{x_i}^n}{dt^2} = A_i - \alpha_i\frac{d{x_i}^n}{dt} \tag{7}$$

where

$$A_i = \frac{1}{m_i}\left(\sum_{\substack{j=1 \\ (j\neq i)}}^{N} F_{xij} + m_i g_x + F_{xi}^{floor}\right) \tag{8}$$

and

$$\alpha_i = \frac{6\pi\eta r_i}{m_i}. \tag{9}$$

Equations (7) and (8) can then be used to simplify Equation (5) to the following form

$$\frac{d{x_i}^n}{dt} = \left(\frac{{x_i}^n - {x_i}^{n-1}}{\Delta t} + \frac{\Delta t}{2}A_i\right)\Big/\left(1 + \alpha_i\frac{\Delta t}{2}\right) \tag{10}$$

Equation (10) can now be evaluated using only ${x_i}^n$ and ${x_i}^{n-1}$. is approximated via :

$${x_i}^1 = {x_i}^0 + \frac{d{x_i}^0}{dt}\Delta t \tag{11}$$

Each time step integration then cycles through the following sequence: evaluate A from Equation (8), solve Equation (10) to give the particle velocities, solve Equation (7) to give the particle accelerations, then solve Equation (6) to find position at the new time step. In this scheme, the force evaluation and solution of the equations of motion are interleaved to overcome the velocity dependence of the force.

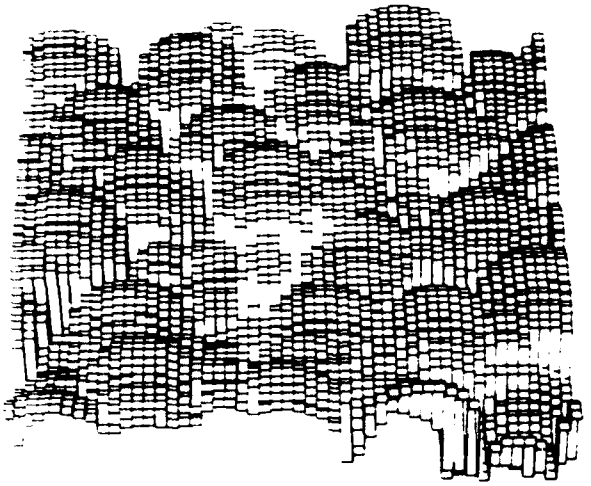

Figure 1. Top surface of the sediment approximated by a grid of squares.

Initially, the particles are placed randomly within a rectangular box and assigned random velocities. Periodic boundary conditions are applied in the X and Y directions, and gravity acts in the negative Z direction. The number of particles in the simulations varied from N=125 to N=1000, and a typical value for the time step was 200μs. Complete sedimentation usually occured within approximately 12,000 to 14,000 cycles. The initial version of the code used a lookup table to evaluate Equation (2), but the MLG version calculated the force at each time step.

In order to compare results for different particle size distributions a method for calculating the sediment volume was required. Given the box dimensions and the particle coordinates and radii, the volume can be calculated by evaluating the volume under the top surface of the particles, and this can be defined by lowering a grid of small squares onto the sediment until all of the squares have intersected a particle. The volume is then the sum of the volumes under every square. Figure (1) shows a typical picture of the top surface of a sediment which has been approximated using this method.

The initial version of the program was designed to run on a VAX 8700 computer and practical limitations restricted the number of particles in the simulation to around N=200 because the CPU time varied as N^2. This is a common problem in MD simulations and arises because in a system of N particles randomly distributed in space the motion of any one particle is in principle determined by the remaining N-1 other particles. In practice however the particle will be influenced significantly by only a relatively small number of nearby particles, defined to be the particles "nearest neighbours", and finding these nearest neighbours in an efficient manner is a central part of any MD simulation.

We redesigned our code to overcome this problem by implementing the MLG algorithm to track near neighbour relationships. The MLG is a data structure in which adjacent particles in space have close grid indices. The data structure is arranged so that a particle's nearest neighbours are readily identified, but without the need to continually calculate the distance to each of the other N-1 particles (an order N operation). The computational cost of the scheme scales as N, and the algorithm is ideally suited to vectorization because it uses data from contiguous memory locations. The MLG has previously been used for a variety of MD simulations of atomic and molecular systems (Lambrakos et al, 1989a,b), but this is the first time it has been applied to macroscopic size particles in a sedimenting system.

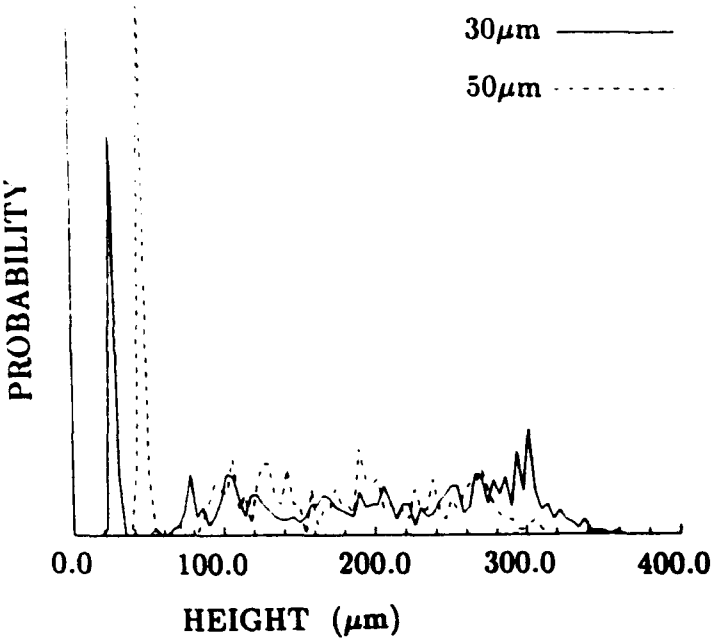

Figure 2a. Probability of finding a particle as a function of height above the floor of the container for the 30/50μm simulation.

3. RESULTS AND DISCUSSION

Initial calculations were performed for suspensions in which all particles had the same radius. Three particle sizes were investigated; r=30, 50 and 100μm, for N=125 or 216. In order to obtain statistically meaningful results six replicate calculations were performed for each radius, the only difference between the calculations being in the starting positions and velocities. A relative density ρ_r, defined as the ratio of sediment density to particle material density, was calculated from the averaged results for each radius value.

If the sedimented material had sufficient time to adjust to an optimum close packed structure we would find $\rho_r = 0.74$, independent of particle size, whereas the simulations gave $\rho_r = 0.72, 0.70, 0.68$ for particle radius values of 30, 50, and 100μm respectively. Thus the packing density was found to be particle size dependent, with an increase in particle size giving a decrease in particle density.

One possible explanation for this lies in the terminal velocities of the particles. By considering the free fall of a particle in the suspension (free fall here means that there are no interparticle or particle/floor forces on the particle) it can be shown that the terminal velocity of a particle is proportional to the square of the particle radius. Hence the smaller particles have a slower terminal velocity and therefore have more time to rearrange and adopt a more efficient structure than the larger particles.

Three different bimodal particle size distributions were investigated; 30/50, 50/100, and 30/100μm mixes. With bimodal distributions there is the possibility of fractionation occuring during sedimentation, and therefore plots of the probability of locating a particle centre as a function of height (in the z direction) were obtained. These are shown in Figure (2).

A common feature of these plots is a pair of well defined, sharp peaks at low heights. For example, the 30/50μm plot (Figure (2a)) has a sharp peak at 26μm for the 30μm particles and another at 46μm for the 50μm particles. These peaks correspond to particles in contact

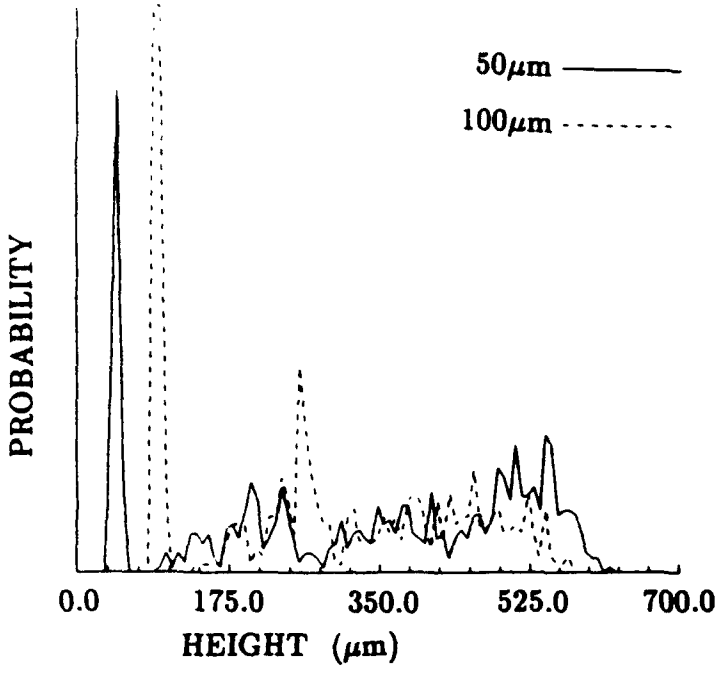

Figure 2b. Probability of finding a particle as a function of height above the floor of the container for the 50/100μm simulation.

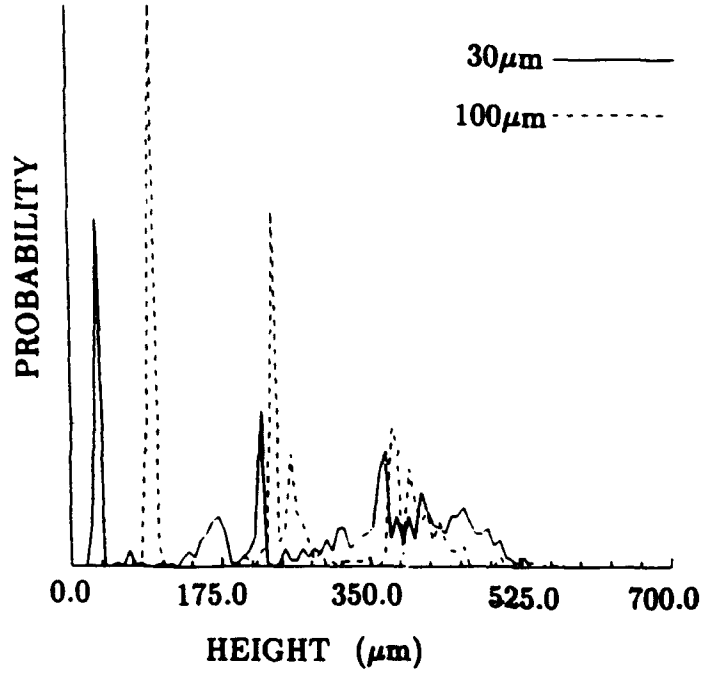

Figure 2c. Probability of finding a particle as a function of height above the floor of the container for the 30/100μm simulation.

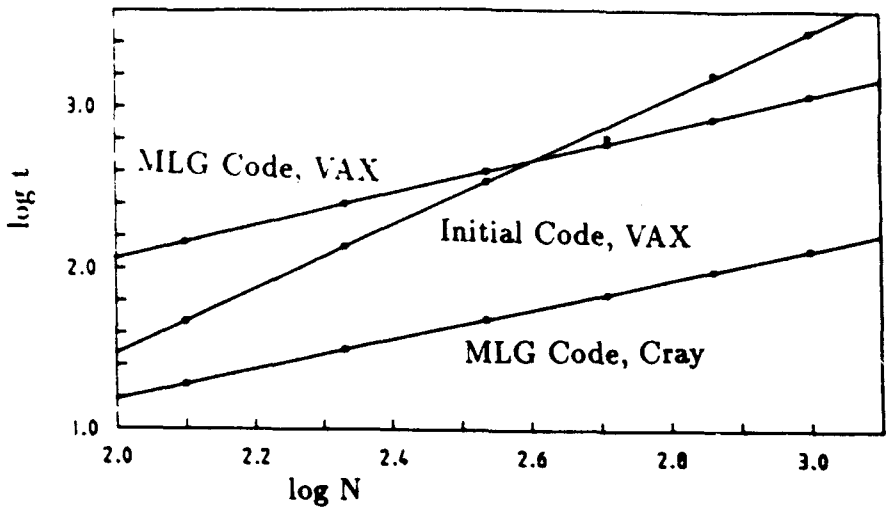

Figure 3. CPU time for 100 cycles versus total number of particles in the simulation.

with the floor of the container. The fact that these peaks occur at heights slightly lower than the corresponding particle radius indicate a small amount of overlap between the floor and the particles (i.e. squashing).

The tendency for the smaller particles to settle after the larger particles is shown by the plots. For the 30/50μm simulation the 30μm probability curve extends out to 360μm whereas the 50μm curve only goes out to 310μm. Thus, beyond 310μm there is zero probability of finding a 50μm particle and only 30μm particles will be found in the range 310μm to 360μm, i.e. a layer of 30μm particles will be formed on the top of the sediment. Similarly, for the 50/100μm simulation (Figure (2b)) 100μm particles are not found above 578μm and only 50μm particles are found between 578μm and 623μm. The 30/100μm simulation (Figure (2c)) is not as clear cut since the probability of finding a 100μm particle above 470μm is not zero, but since it is very small we can take 470μm as the upper limit for the 100μm particles here. Only 30μm particles will be found between 470μm and 530μm.

The bimodal results were obtained using either N=216 or N=512, with the larger number of particles being run on the MLG version of the code. We also ran a series of simulations using up to 1000 particles to check the order N scaling of the MLG on both the VAX 8700 and a Cray X-MP. Plots of CPU time for 100 cycles versus total number of particles are shown in Figure (3) for both the original version of the code and the MLG version on both the VAX and the Cray.

The original code shows the N^2 dependency (gradient equals 1.98), while the MLG code on the VAX shows a linear dependence on N (gradient equals 1.08), as expected. It is interesting to note that the MLG code on the VAX takes longer to run 100 cycles than does the original version of the code when small particle numbers are used. This is not unexpected because of the additional initial computational overheads associated with the MLG, and the repeated use of Equation (2) instead of a lookup table. Crossover occurs around N=500, and for N=1000 the MLG version is more than twice as fast.

The MLG code when run on the Cray also shows a linear dependence on N (gradient equals 0.97) and considerably reduced CPU times. The speedup is only marginally better than that due to the faster clock rate on the Cray however, indicating that little vectorisation is occuring, and this is due to the relatively small number of particles we are using. In an

MLG code the N particles are specified by assigning values to three numbers: NX, NY, and NZ, where $N = NX \times NY \times NZ$. In a "regular" MLG structure the computationally intensive parts of the code are contained within a nested set of DO loops over indices i, j, and k, which vary between 1 and NX, NY, and NZ respectively. For 1000 particles we have NX = NY = NZ =10, which means that the innermost loop has a count of only 10, which is far too short for the increase in speed due to the pipeline architecture to be effective.

4. CONCLUSION

For monomodal particle size distributions the MD results show that the packing density is particle size dependent, with an increase in particle radius giving a decrease in sediment density. For bimodal distributions fractionation was found to occur and a layer of smaller particles formed on the top of the sediment. This type of inhomogeneity has important consequences for the sensitivity and mechanical properties of an explosive where sedimentation may have occurred during production. Use of the regular MLG algorithm reduced the N^2 dependency on CPU time to order N, but further improvements in efficiency require the use of either larger particle numbers or a "skew-periodic" MLG on a vector compiler (Lambrakos and Boris, 1987), or the application of the regular MLG on a massively parallel computer (Phillips, 1991).

5. REFERENCES

Bossis, B., and Brady, J.F., (1984), *Dynamic simulation of sheared suspensions. 1. General method.* Journal of Chemical Physics, **80**, 5141-5154.

Boris, J.P. (1986), *A vectorized near neighbors algorithm of order N using a monotonic logical grid*, Journal of Computational Physics, **66**, 1-20.

Lambrakos, S.G., and Boris, J.P., (1987), *Geometric properties of the monotonic lagrangian grid algorithm for near neighbor calculations.*, Journal of Computational Physics, **73**, 183-202.

Lambrakos, S.G., Boris, J.P., Guirguis, R., Page, M., and Oran, E.S., (1989a), *Molecular dynamics simulation of* $(N_2)_2$ *formation using the monotonic lagrangian grid*, Journal of Chemical Physics, **90**, 4473-4481.

Lambrakos, S.G., Peyrard, M., Oran, E.S., and Boris, J.P., (1989b), *A new approach to molecular dynamics simulations of shock-induced detonations in solids*, Physical Review B, **39**, 993-1005.

Phillips, L., Oran, E.S., and Boris, J.P., (1991), *Molecular Dynamics of Shocks in Crystals with Defects*, preprint.